TfR2 localizes in lipid raft domains and is released in exosomes to activate signal transduction along the MAPK pathway

Alessia Calzolari[1], Carla Raggi[2], Silvia Deaglio[3], Nadia Maria Sposi[1], Marit Stafsnes[1], Katia Fecchi[2], Isabella Parolini[1], Fabio Malavasi[3], Cesare Peschle[1], Massimo Sargiacomo[2] and Ugo Testa[1,*]

[1]Department of Hematology, Oncology and Molecular Medicine and [2]Department of Pharmacology, Istituto Superiore di Sanità, Viale Regina Elena 299, 00161 Rome, Italy
[3]Laboratory of Immunogenetics, Department of Genetics, Biology, and Biochemistry, University of Turin Medical School, Via Santena 19, 10125 Turin, Italy
*Author for correspondence (e-mail: u.testa@iss.it)

Accepted 1 August 2006
Journal of Cell Science 119, 4486-4498 Published by The Company of Biologists 2006
doi:10.1242/jcs.03228

Summary

Transferrin receptor 2 (TfR2) possesses a YQRV motif similar to the YTRF motif of transferrin receptor 1 (TfR1) responsible for the internalization and secretion through the endosomal pathway. Raft biochemical dissection showed that TfR2 is a component of the low-density Triton-insoluble (LDTI) plasma membrane domain, able to co-immunoprecipitate with caveolin-1 and CD81, two structural raft proteins. In addition, subcellular fractionation experiments showed that TfR1, which spontaneously undergoes endocytosis and recycling, largely distributed to intracellular organelles, whereas TfR2 was mainly associated with the plasma membrane. Given the TfR2 localization in lipid rafts, we tested its capability to activate cell signalling. Interaction with an anti-TfR2 antibody or with human or bovine holotransferrin showed that it activated ERK1/ERK2 and p38 MAP kinases. Integrity of lipid rafts was required for MAPK activation. Co-localization of TfR2 with CD81, a raft tetraspanin exported through exosomes, prompted us to investigate exosomes released by HepG2 and K562 cells into culture medium. TfR2, CD81 and to a lesser extent caveolin-1, were found to be part of the exosomal budding vesicles. In conclusion, the present study indicates that TfR2 localizes in LDTI microdomains, where it promotes cell signalling, and is exported out of the cells through the exosome pathway, where it acts as an intercellular messenger.

Key words: Transferrin, Iron metabolism, Lipid rafts, Cell signalling

Introduction

Ever since it was cloned, transferrin receptor 2 (TfR2), a new TfR-like family member, was thought to mediate a new pathway of iron uptake (Glockner et al., 1998; Kawabata et al., 1999). Like TfR1, TfR2 binds diferric Tf at neutral pH and apo Tf at acidic pH (Kawabata et al., 2000). TfR2, whose physiological role remains elusive, has been found to be predominantly expressed in the liver (Fleming et al., 2000; Deaglio et al., 2002) and intestine (Griffiths and Cox, 2003), but is commonly studied in model systems, such as erythroleukemia K562 and hepatoblastoma HepG2 cell lines (Kawabata et al., 1999). Stably transfected human TfR2 increases Tf binding and iron uptake in cells (Kawabata et al., 2000). Mutations of the TfR2 gene result in hemochromatosis type 3, associated with the development of significant hepatic iron loading (Camaschella et al., 2000; Roetto et al., 2002). TfR2 knockout mice develop iron overload typical of TfR2-associated hemochromatosis (Wallace et al., 2005). To explain the hepatic iron overload observed in type 3 hemochromatosis and in TfR2-KO mice it was hypothesized that TfR2 acts as an iron sensor in the liver to regulate the rate of the synthesis of hepcidin, itself a central regulator of iron metabolism (Kawabata et al., 2005; Nemeth et al., 2005).

The expression pattern of TfR2 is quite different from TfR1 in that TfR2 is detected mainly in the liver, whereas TfR1 is widely expressed in the various tissues, with a preferential expression at the level of the erythroid lineage and of the rapidly dividing tissues (Kawabata et al., 1999). TfR2 expression is increased by iron loading, whereas TfR1 expression is downregulated (Johnson and Enns, 2004; Robb et al., 2004). The same is true during liver development where TfR2 is upregulated and TfR1 is downregulated (Robb et al., 2004). However, during erythroid differentiation of murine erythroleukemia (MEL) cells induced by dimethylsulfoxide, expression of TfR1 increases, whereas TfR2 decreases (Kawabata et al., 2001). In MEL cells, expression of TfR1 is induced by desferrioxamine, an iron chelator, and it is reduced by ferric nitrate. By contrast, levels of TfR2 are not affected by the cellular iron status (Kawabata et al., 2001).

Nevertheless, human TfR1 and TfR2 are very similar, being 45% homologous and 60% similar in their primary structure (Kawabata et al., 1999). Functional attributes of these similarities apply to their Tf-binding properties (ligand binding RGD structure) and in the peptide encompassing the internalization/exosomal-sorting motif present in the cytoplasmic tail of the two receptors (YTRF for TfR1 and YQRV for TfR2). The presence of this internalization/exosomal-sorting motif positions the two receptors at similar

cellular sites, where internalization of the plasma membrane through endosomal sorting complex is achieved. In this context, a recent study indicates that Tf delivered through both receptors was initially observed at the plasma membrane and in tubulovesicular endosomes; however, at later stages of the internalization process Tf internalized through the TfR2 is delivered to multivesicular bodies, whereas Tf endocytosed through the TfR1 does not transit in this compartment (Robb et al., 2004).

In a first set of experiments we have evaluated the localization of TfR2 at the level of membrane microdomains. We found that TfR2 was mainly localized within the low-density Triton-insoluble (LDTI) fractions of both HepG2 cells and K562 cells expressing caveolin-1 (K562cav), whereas TfR1, as expected, was excluded from these fractions. Confocal microscopy further suggested co-localization of TfR2 and caveolin-1 in HepG2 cells; interestingly, TfR2 also co-localized with the tetraspanin CD81, a lipid-raft-resident protein exported through exosomes. This result prompted us to investigate the exosomes released into K562 and HepG2 cell media. TfR2, together with TfR1, CD81 and low levels of caveolin-1 were found to be part of the exosomal budding vesicles. Immunoprecipitation experiments allowed us to assess for the first time an interaction between TfR2 and the two raft proteins caveolin-1 and CD81 in LDTI fractions collected from HepG2 cells and K562cav cells.

Given the localization of TfR2 in cell membrane microdomains specialized in cell signalling, it seemed logical to evaluate the capacity of this membrane receptor to activate cell signalling. In erythroleukemia K562 cells, following interaction with anti-TfR2 monoclonal antibody or with holotransferrin, the activation of ERK1/ERK2 (extracellular signal-regulated kinases 1/2) and p38 MAP kinases was observed independently of the caveolin-1/TfR2 interaction. Lipid raft integrity was strictly required for TfR2-mediated MAPK activation.

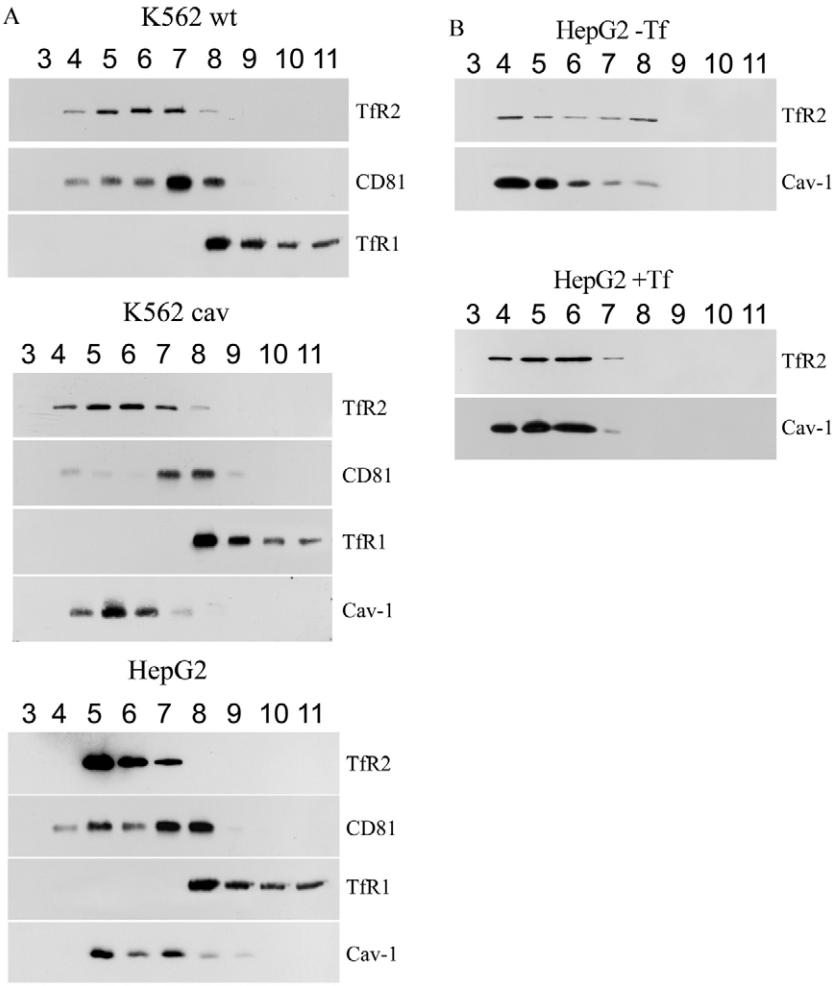

Fig. 1. Association of TfR2 with lipid rafts/caveolae by density gradient centrifugation. (A) K562 cav, K562 wt and HepG2 cells were lysed in Triton X-100 and subjected to sucrose gradient centrifugation. Aliquots of fractions collected from the top of the gradient were analyzed by western blotting with the antibodies against TfR2, CD81, TfR1 and caveolin-1. Equal protein amounts for each fraction were resolved by SDS-PAGE. (B) HepG2 cells were serum-starved overnight and subjected to sucrose gradient centrifugation (top panels). In a second set of experiments, serum-starved HepG2 cells were pre-treated with human holotransferrin (4 hours at 37°C), before sucrose gradient and western blot analysis.

Results

TfR2 is constitutively localized in lipid raft cell compartments and associates with caveolin-1

Sucrose density gradient ultracentrifugation of cell lysates was used to purify lipid raft microdomains, which are resistant to solubilization with non-ionic detergents at low temperature, because of their cholesterol- and glycosphingolipid-rich composition.

After sucrose gradient centrifugation, detergent-resistant lipid rafts float to low-density fractions because of their high lipid content. These insoluble membranes, visible as a white opalescent band in fractions 4, 5 and 6, were compared with soluble fractions 8-11 for TfR2 content. Immunoblot analysis performed by SDS-PAGE loaded with equal amount of protein for each fraction showed that TfR2 was predominantly located in insoluble fractions both in HepG2 and in stably transfected K562cav cells. As expected, caveolin-1, which was used to track the position of caveolae-enriched membranes, was detected in detergent-resistant insoluble fractions (Fig. 1A). Interestingly, the gradient distribution of TfR2 was identical both in K562wt and K562cav cells (Fig. 1A), indicating that caveolin-1 is not required for the localization of TfR2 in lipid rafts. As expected, the raft-resident protein CD81 was detected in Triton X-100 insoluble fractions, whereas the non-raft marker TfR1 was localized in soluble fractions 9-11 (Fig. 1A).

In a second set of experiments, we compared the gradient distribution of TfR2 in serum-starved HepG2 cells (in the absence of exogenous transferrin) and in holotransferrin-exposed HepG2 cells (Fig. 1B, top and bottom panels, respectively). The results indicated that in Tf-stimulated

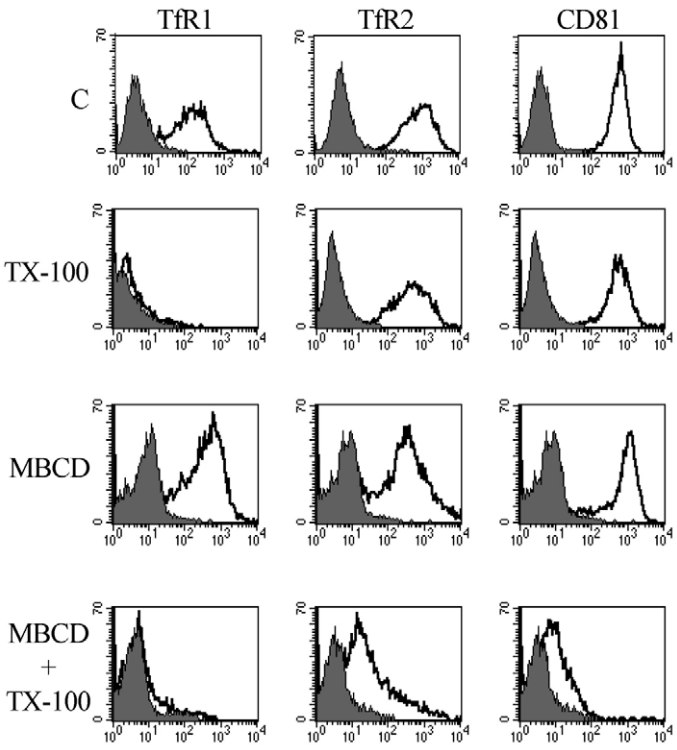

Fig. 2. Effect of Triton X-100 treatment and cholesterol depletion on TfR2 and TfR1 cell membrane expression. K562 cells were labeled with anti-TfR1, anti-TfR2 or anti-CD81 mAbs (left, middle and right panels, respectively) and the fluorescence was measured before (C) and after (TX-100) 5 minutes of detergent treatment. Depletion of plasma membrane cholesterol was achieved by incubation with methyl-β-cyclodextrin (MBCD) before antibody labeling and TX-100 treatment.

HepG2 cells, TfR2 is more concentrated in low-density insoluble fractions (4, 5 and 6), perfectly reflecting the caveolin-1 concentration, whereas in Tf-starved cells TfR2 was diffused between fractions 4-8.

The predominant compartmentalization of TfR2 at the level of caveolae-enriched microdomains was also proved by a flow cytometric test for detecting raft association of membrane proteins. In this assay, detergent-sensitive plasma membrane proteins are rapidly dissolved by low concentrations (i.e. 0.2%) of non-ionic detergents that do not affect cellular integrity, whereas lipid-raft-associated proteins show high resistance to this treatment (Gombos et al., 2004). However, following disruption of lipid rafts by cholesterol depletion via incubation with methyl-β-cyclodextrin (MBCD), raft-associated proteins are released by detergent treatment. The analysis performed on K562 cells first labeled with anti-TfR2, anti-CD81 or anti-TfR1 antibodies and then treated with 0.2% Triton X-100 (TX-100) indicated that TX-100 treatment did not affect the TfR2 and CD81 labeling, whereas it almost completely abrogated TfR1 labeling (Fig. 2). In a second set of experiments, cells were depleted of plasma membrane cholesterol by incubation with MBCD, which is known to affect lipid raft integrity, then labeled with anti-TfR2, anti-TfR1 and anti-CD81 monoclonal antibodies and finally treated with detergent. After selective destabilization or disruption of the rafts by MBCD cholesterol depletion, TfR2 as well as CD81 labeling underwent a net decrease (Fig. 2), indicating that the observed detergent resistance of TfR2 is consistent with lipid raft localization.

To confirm the immunoblot data concerning the plasma membrane localization of TfR2, we performed immunofluorescence double staining to localize TfR2 and the raft-resident caveolin-1 protein. In HepG2 cells TfR2 and caveolin-1 largely co-localized in the plasma membrane (Fig. 3A). It is of interest to note that the TfR2 labeling pattern was quite similar to that of tetraspanin CD81, a raft-resident protein (Fig. 3B). In parallel, double-labeling experiments with anti-TfR1 and anti-caveolin-1 provided evidence that these two proteins do not co-localize at the level of the cell membrane, although some membrane regions showed the juxta-apposition of these two proteins (Fig. 3C). Detergent treatment (1% TX-100) of stained HepG2 cells clearly showed a loss of TfR1 labeling, whereas TfR2 (Fig. 3D) and CD81 (data not shown) labeling remained virtually unmodified in its intensity and the surface fluorescence showed a more mottled appearance after detergent extraction (Fig. 3D).

Given the limited resolution of light microscopy, these experiments suggest a possible association between TfR2 and caveolin-1, which needs to be proved by immunoprecipitation experiments. We therefore carried out immunoprecipitation experiments with LDTI or whole cell extracts isolated from HepG2 and K562 cav cells whose surface plasma membrane proteins were covalently biotinylated with the impermeant probe sulfo-N-hydroxy-succinimmido-biotin (sulfo-NHS-biotin) (Sargiacomo et al., 1989). Both TfR1 and TfR2 were labeled with biotin, whereas cytoplasmically oriented caveolin-1 was not accessible to the reagent. The outcome of the immunoprecipitation of HepG2 with anti-TfR2 or anti-TfR1 mAbs, loaded on SDS-PAGE and immunoblotted with streptavidin-horseradish peroxidase (strept) or with both TfRs and caveolin-1 is shown in Fig. 3E,F. The results clearly demonstrated that among the multitude of biotinylated proteins only the TfR molecules appeared to be decorated with streptavidin as a consequence of the immunoprecipitation and that caveolin-1 was only co-immunoprecipitated by the anti-TfR2. The same results were obtained in K562 cav cells (data not shown).

Intracellular pool of TfR2

Previous studies, carried out in K562 (Watts, 1985) and HeLa cells (Lamb et al., 1983) clearly show that TfR1, even in the absence of its ligand, is rapidly internalized: as a consequence of this phenomenon a significant proportion (30-60%) of total TfR1 is localized in intracellular pools. We therefore determined the proportion of TfR1 and TfR2 present in cell membranes and intracellular pools, respectively, in K562 and HepG2 cells. To perform this analysis, we incubated K562 cells with trypsin at 4°C, to cleave the cell-surface-bound TfR1 and TfR2. Following this treatment, both receptors almost completely disappeared from the cell membrane, as shown by flow cytometry performed on intact cells (Fig. 4A). On the contrary, flow cytometry carried out on fixed and permeabilized cells, to allow the intracellular labeling of the receptors, showed that in trypsin-treated cells, significant reactivity remained with anti-TfR1, but it was low with anti-TfR2 (Fig. 4B). In parallel, western blot analysis performed on

untreated and trypsinized K562 cells provided evidence that the intracellular portion of total TfR1 is about 30-40%, whereas it decreased to about 5% for TfR2 (Fig. 4B). Similarly, western blot analysis performed on total cellular lysates of both untreated and trypsinized HepG2 cells basically showed results comparable with those obtained from K562 cells. Immunoblotting with anti-caveolin-1 was included as a control of trypsin treatment specificity (Fig. 4C).

Previous studies (Lamb et al., 1983) show that a portion (about 20%) of the intracellular TfR1 pool is insensitive to trypsin treatment at 37°C, suggesting that this portion does not recycle to the cell surface. To confirm these data and to verify whether this phenomenon could occur for TfR2, we incubated K562 cells with trypsin at 37°C for 20 minutes. Western blot analysis of trypsinized cells showed that about 10% of TfR1 was insensitive to the treatment, whereas TfR2 was undetectable after trypsin digestion at 37°C, indicating that during the experimental time period all TfR2 recycled to the cell surface (Fig. 4D).

To analyze the subcellular localization of TfR2 biochemically, we performed subcellular fractionation of K562 cells. Post-nuclear supernatants were prepared from K562 cells and fractionated on a discontinuous sucrose gradient, and the distribution of TfR2 within the gradient was compared with the plasma membrane or early endosomal Rab5 protein, the early endosomal and recycling endosomal Rab11 protein, with the late endosomal and lysosomal membrane protein Lamp-2, with the Golgi apparatus protein marker Golgin-97 and with the membrane and early endosomal and recycling endosomal membrane protein TfR1. TfR2 immunoreactivity was mainly detected in fractions 1 and 2, coincident with Rab5 and in part TfR1 (Fig. 5). TfR1 was mainly detected in fractions 2 and 3, coincident with Rab5 and Rab11. In particular, a large part of TfR1 immunoreactivity co-sedimented with an endosomal Rab11^{+}/Rab5^{-} fraction, corresponding to recycling endosomes, as previously reported (Trischler et al., 1999). Lamp-2 and Golgin-97 appeared in different locations to TfR2.

Thus, the observations in our subcellular fractionation studies suggested that TfR2 was

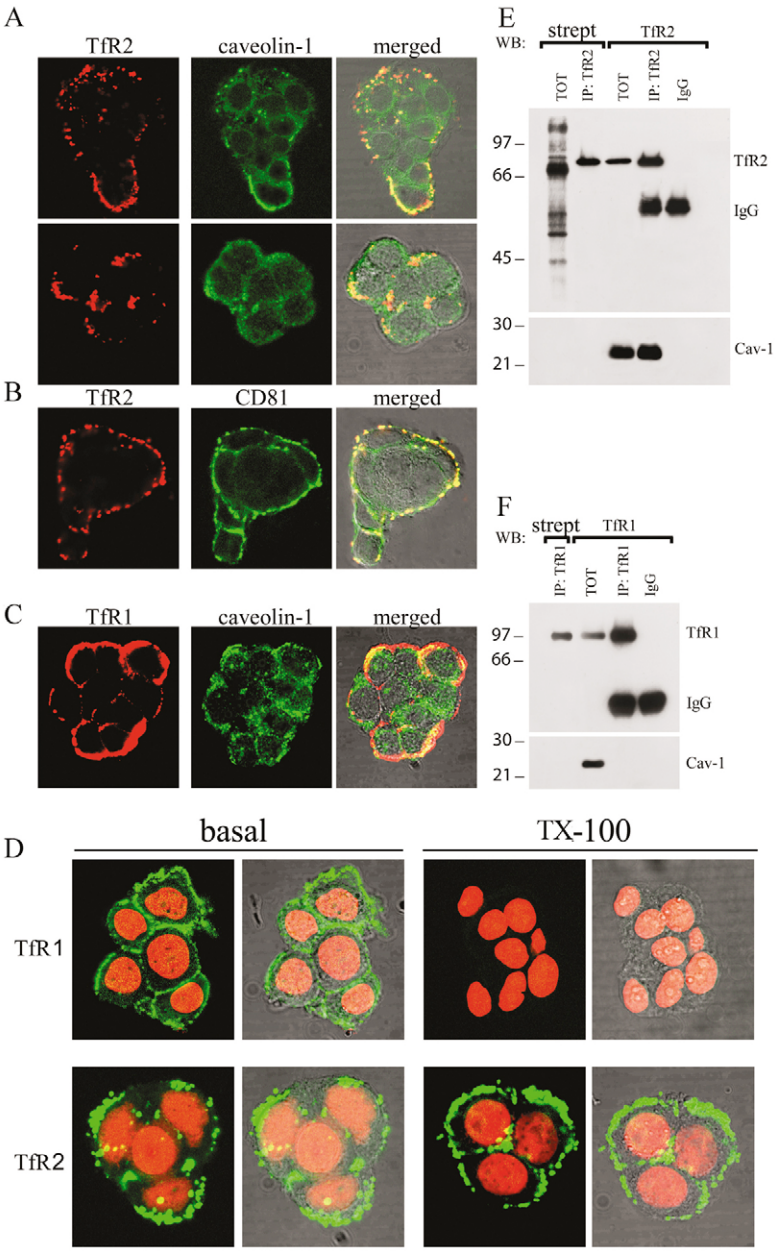

Fig. 3. Association between TfR2 and caveolin-1 in LDTI membranes as shown by immunofluorescence and immunoprecipitation experiments. (A) HepG2 cells were plated on coverslips and left to adhere overnight. Cells were stained with a mouse mAb directed against TfR2, followed by a Texas-Red-conjugated goat anti-mouse IgG. Cells were then fixed with paraformaldehyde (PFA, top panels) or with methanol/acetone (bottom panels), permeabilized and stained with a rabbit polyclonal anti-caveolin-1, followed by a FITC-conjugated anti-rabbit IgG. (B) HepG2 cells were stained with anti-TfR2 (red), then fixed (PFA) and labeled with a FITC-conjugated anti-CD81 mAb. (C) HepG2 cells were labeled with anti-TfR1 mAb, followed by a Texas-Red-conjugated goat anti-mouse IgG. Cells were then fixed and permeabilized (methanol/acetone, saponin) and stained with a rabbit polyclonal anti-caveolin-1, followed by a FITC-conjugated anti-rabbit IgG. (D) HepG2 cells were stained using the indicated primary mAbs, followed by a FITC-conjugated goat anti-mouse IgG. Where indicated, stained cells were exposed to Triton X-100 (TX-100) before analysis. Nuclei were counterstained using Syto59. (E) LDTI domains prepared from biotinylated HepG2 cells were immunoprecipitated with anti-TfR2 mAb. Top panel shows detection of immunoprecipitated (IP) and total (TOT) LDTI by anti-TfR2 or by streptavidin-horseradish peroxidase conjugated (strept). Bottom panel shows detection of IP and total LDTI by anti-caveolin 1 antibody. Only externally exposed biotinylated proteins were detected by streptavidin-HRP. As a control, an irrelevant antibody was used for immunoprecipitation (IgG). Positions of molecular size markers in kDa are indicated on the left. (F) Whole cell extracts prepared from biotinylated HepG2 cells were immunoprecipitated with a mouse mAb directed against TfR1. Total lysate (TOT) and immunoprecipitated fraction (IP) were detected by streptavidin-HRP-conjugated (strept) anti-TfR1 (top panel) and by anti-caveolin-1 (bottom panel). As a control, an irrelevant antibody was used for immunoprecipitation (IgG).

expressed mainly at the level of the plasma membrane and within the early endosomal membranes.

TfR2 is a component of exosomes released from HepG2 and K562 cells and associates with CD81 in LDTI microdomains

Given the results showing the co-localization between TfR2 and CD81 and because many tetraspanin proteins (CD9, CD63, CD81, CD82), which form a protein web displaying affinity for detergent-resistant domains, are found to be enriched in exosomes (Escola et al., 1998), we investigated the expression of TfR2 in exosomes obtained from K562 wt, K562 cav and HepG2 cells and compared their protein content with that of LDTI extracted by the same cells. To investigate this issue we first developed a domain-selective biotinylation-streptavidin blotting strategy to determine the degree by which plasma membrane (PM), LDTI and exosomes, once separated, differ in protein patterns and sucrose buoyancy (Fig. 6). The capacity of exosomes to float at light densities on sucrose gradient is an accepted criterion to distinguish membrane vesicles purified as exosomes from cellular debris and apoptotic blebs (Théry et al., 2001). The results showed how cellular debris containing biotinylated PM and exosomes float differently in a sucrose density gradient. Note that PM proteins of cell debris floated on fractions corresponding to sucrose density 1.15-1.19 g/ml (fractions 9-11), whereas exosomes mostly floated on lighter sucrose fractions corresponding to sucrose density of 1.10-1.16 g/ml (fractions 4, 5, 6) (Fig. 6A,B), as indicated by the distribution of the exosome marker Lamp-2. Interestingly, TfR2 distribution was found to perfectly match that observed for Lamp-2. In accordance with other studies (Gutwein et al., 2005) we found that exosome preparation include also heavier vesicles, ranging from fraction 7 to 11, devoid of exosomal-lysosomal markers, probably representing membrane blebs (Fig. 6B). In subsequent experiments we used exosome preparations derived from pooled fractions 4-6. In addition, the results reported in Fig. 6C (left panel) showed differences in NHS-biotin-labeled proteins between the specific cellular compartments (PM, LDTI and exosomes). Furthermore, in agreement with other papers, exosomes were shown to express TfR1 (Savina et al., 2002; Savina et al., 2003), but not CD45 (Nguyen et al., 2003; Blanchard et al., 2002) (Fig. 6C, right panel).

The biochemical characterization of K562 and HepG2

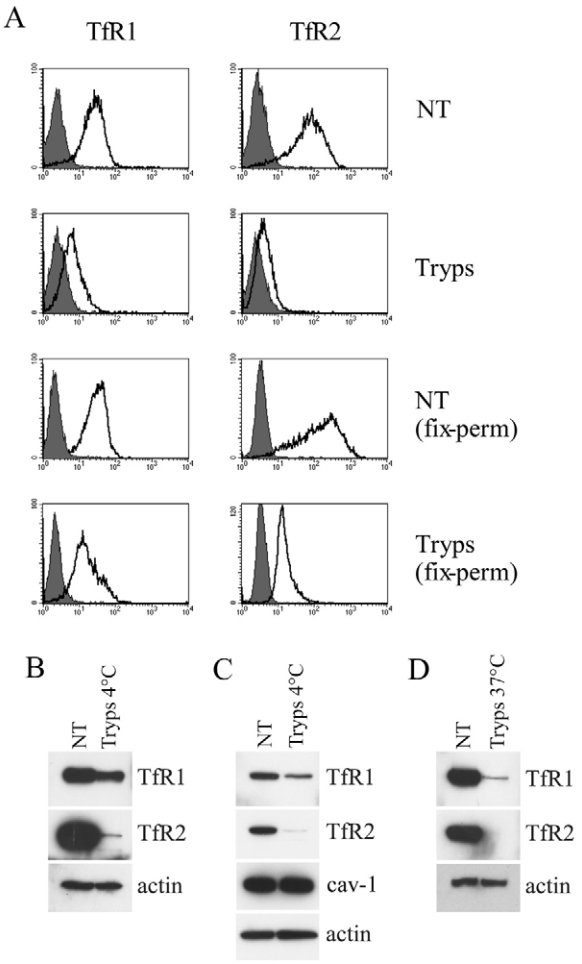

Fig. 4. Surface and intracellular distribution of TfR1 and TfR2. (A) K562 cells were incubated at 4°C for 1 hour with either PBS (untreated cells, NT) or PBS containing trypsin (trypsinized cells, Tryps). For flow cytometry analysis, labeling with anti-TfR1 and anti-TfR2 was performed on intact cells and on fixed and permeabilized cells (fix-perm). (B-D) Aliquots of untreated (NT) and trypsinized (Tryps) K562 (B,D) or HepG2 (C) cells (4°C or 37°C) were lysed and total cellular lysates were resolved by SDS-PAGE and immunoblotted against TfR1, TfR2 and caveolin-1. Blots were stripped and reprobed for actin to ensure equal protein loading and transfer.

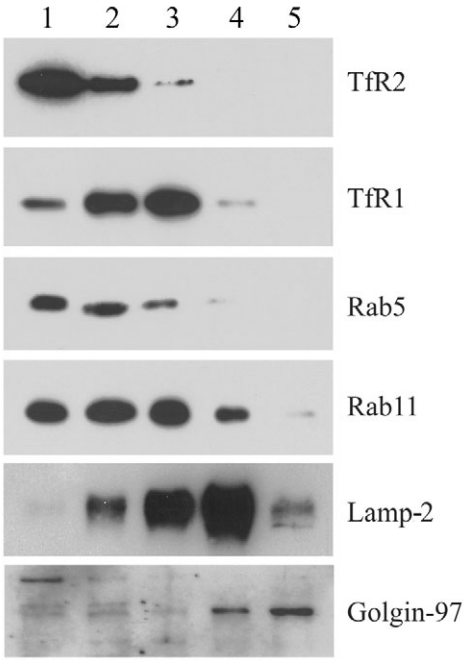

Fig. 5. Subcellular fractionation of K562 cells. K562 cells were broken by nitrogen cavitation and the resulting lysate was clarified by centrifugation. The postnuclear supernatant was layered over the top of a sucrose density gradient and centrifuged (30,000 rpm, 2 hours). The four fractions and the pellet (fraction 5) were collected from the top of the tube and characterized by western blot using antibodies directed against TfR2, TfR1, Rab5, Rab11, Lamp-2 and Golgin-97.

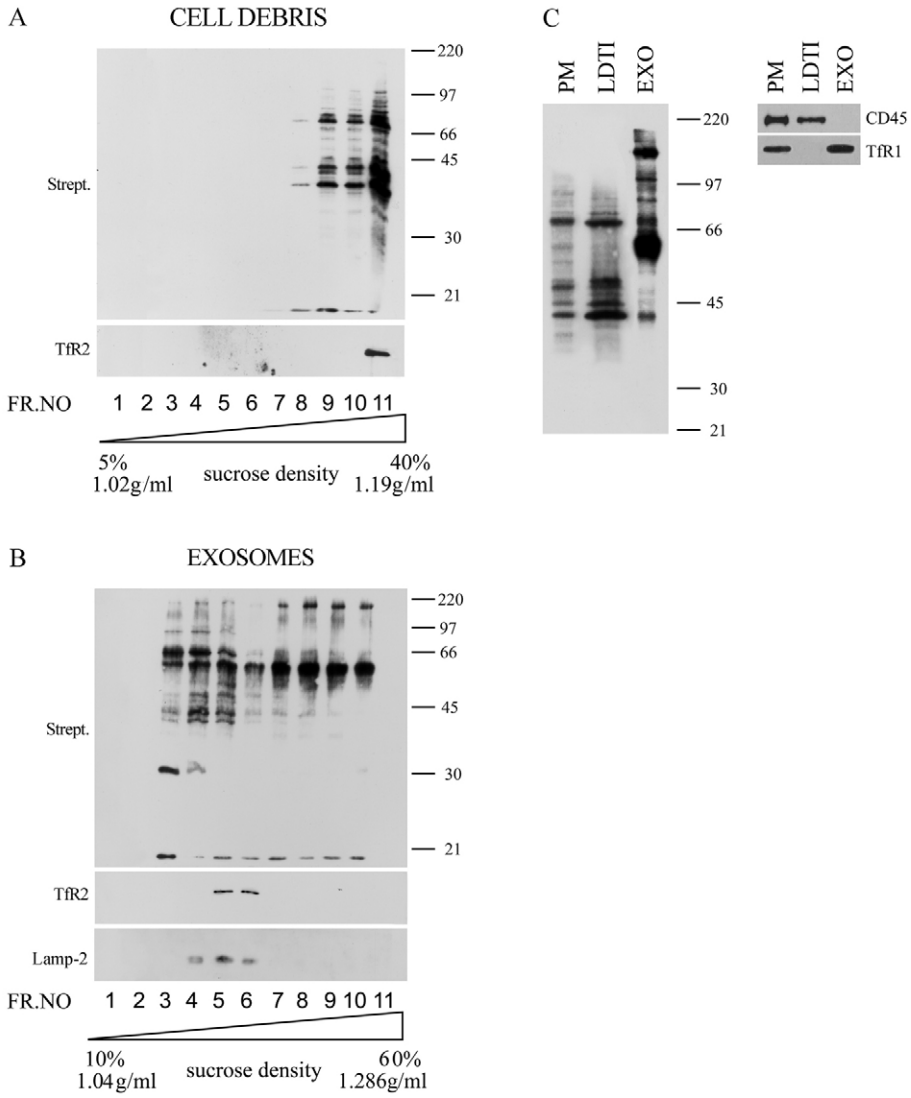

Fig. 6. Analysis of exosomes isolated from K562 cav cell culture media. (A) 20 μg cell debris obtained by centrifugation of culture medium from biotinylated-K562 cav cells was subjected to a 40%-5% continuous sucrose gradient in the absence of detergent, then analyzed by streptavidin and TfR2 immunoblotting. Positions of molecular size markers in kDa are indicated on the right. (B) 20 μg exosomes obtained as described in Materials and Methods were biotinylated then layered on a 30% to 10% continuous sucrose gradient and analyzed by streptavidin and TfR2 immunoblotting. In both cases equal volumes of fractions 1-11 were loaded. Sucrose densities were obtained for each fraction by refractometry. (C) Left panel, 3 μg of plasma membrane (PM) and 3 μg of LDTI prepared from biotinylated K562 cav cells or 1 μg of biotinylated exosomes (EXO) from K562 cav cells were analyzed by streptavidin immunoblotting. Note the differential pattern of biotinylated proteins displayed as exosomes, LDTI and PM. Right panel, equal protein amounts of plasma membrane (PM), LDTI and exosomes (EXO) prepared from K562 cav cells were analyzed by western blotting for CD45 and TfR1 expression.

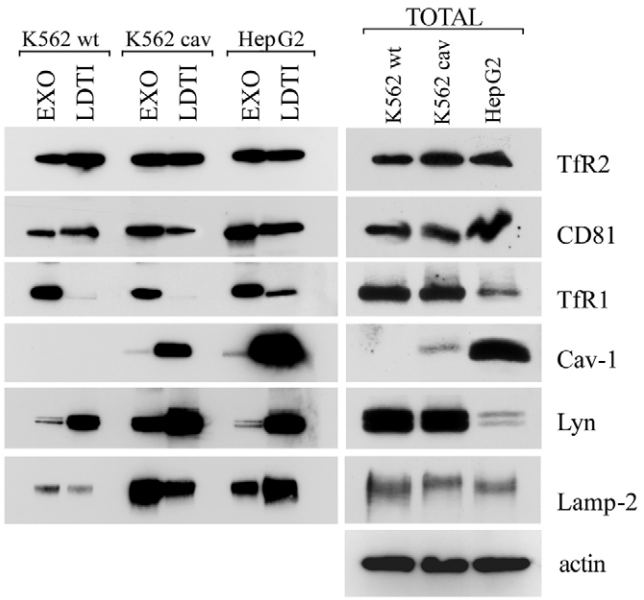

derived LDTI and exosomes indicated that TfR2 appeared at the same time a marker of both LDTI and exosomes, as well as the tetraspanin CD81, the Src tyrosine kinase Lyn and the exosome/lysosome membrane marker Lamp-2 (Fig. 7), i.e. proteins which were previously shown to be secreted in exosomes (Théry et al., 2001). On the contrary, the non-raft marker TfR1 was found to be highly enriched in exosomes and, in agreement with the literature (De Gassart et al., 2003), traces of TfR1 were found in the LDTI fractions. The caveolar marker caveolin-1 was also found to be minimally secreted in exosomal vesicles (Fig. 7). Low amounts of caveolin-1 might be exported through the exosomal pathway

Fig. 7. Biochemical characterization of exosomes derived from K562 and HepG2 cells. Equal protein amounts of exosomes (EXO) and LDTI (left panel) or total cellular lysates (right panel) obtained from K562 wt, K562 cav and HepG2 cells were resolved by SDS-PAGE and immunoblotted with the use of antibodies for TfR2, CD81, TfR1, caveolin-1, the raft-marker Lyn, the exosomal-lysosomal marker Lamp-2, and actin to demonstrate equivalent protein loading and transfer.

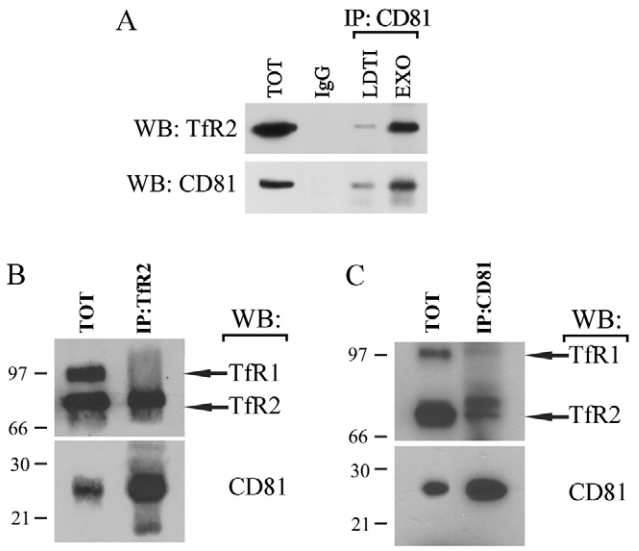

Fig. 8. Association between CD81 and TfR2 in LDTI membranes and exosomes. (A) 40 μg of exosomes (EXO) and 10 μg of LDTI purified from K562 cav cells were immunoprecipitated with an anti-CD81 mAb, resolved by SDS-PAGE under non-reducing conditions and immunoblotted against TfR2 and CD81. As a control of antibody specificity, non-immune serum (IgG) was used to immunoprecipitate the lysates. (B) Exosomes prepared from K562 cav cell culture medium were incubated with beads coated with anti-TfR2 mAb in the absence of detergents; the purified $TfR2^+$ exosomes (IP with TfR2) were then lysed and immunoblotted against TfR2, TfR1 and CD81. (C) K562-derived exosomes were immunoprecipitated with anti-CD81 mAb (IP with CD81) and stained with mAbs for TfR2, TfR1 and CD81. One aliquot of total exosomal lysate (TOT) was loaded as a control.

as a result of sorting owing to TfR2–caveolin-1 association in the rafts.

We next investigated whether a physical interaction between CD81 and TfR2 might occur. Thus we performed a co-immunoprecipitation experiment on LDTI and exosomes purified from K562 cav cells (Fig. 8A). As a result, CD81 was demonstrated to be associated with TfR2 in either LDTI or exosomal samples. Similar results have been obtained in K562 wt and HepG2 cells (data not shown).

Since both TfRs are secreted in exosomes, we determined whether they are present on the same or on distinct vesicles. To do so, we incubated exosomes purified from K562 cav cells with beads coated with anti-TfR2 mAb in the absence of detergents, we then lysed the purified TfR2-expressing exosomes and analyzed their CD81 and TfR1 content by immunoblotting: these $TfR2^+$ exosomes were shown to express CD81, but not TfR1 (Fig. 8B). Furthermore, we incubated exosomes with anti-CD81 mAb and stained these CD81-expressing exosomes with anti-TfR2 and anti-TfR1, providing evidence that they contain TfR2, but not TfR1 (Fig. 8C).

TfR2 content in LDTI and exosomes

Since TfR2 is expressed in LDTI and exosome preparations, we analyzed the proportion of total cellular TfR2 present in LDTI versus the amount secreted in exosomes. To do so, we used western blotting to determine the amount of the receptor in whole cell lysates, LDTI and exosomes prepared from a given number (10×10^6) of K562 wt and K562 cav cells. The results of this analysis, reported in Table 1, indicated that: (1) ~10% of TfR2 is released in exosomes, which represent about 1% of total cell protein; (2) ~50% of TfR2 is present in LDTI, which represent about 2% of total cell protein. These data clearly show that TfR2 is highly enriched in both LDTI and exosomes, independently of the presence of caveolin-1.

Table 1. Total protein and TfR2 content of K562 cells

	Total protein content (mg)		TfR2 content (AU)*	
	K562 wt	K562 cav	K562 wt	K562 cav
Whole cell lysate	1640±391	1700±297	750±88	740±82
LDTI	35±5.6	29±4.4	413±62	344±55
Exosomes	19±4.2	16±3.5	114±21	94±16

*TfR2 content was evaluated after western blot analysis of whole cell lysate, LDTI and exosome preparations and after densitometry analysis the results were referred to 10×10^6 cells. Mean values ± s.e.m. observed in three separate experiments are reported.

TfR2 leads to MAPK activation

Since the experiments reported above have shown the localization of TfR2 at the level of lipid rafts and since these membrane microdomains play an important role in signal transduction (Simons and Toomre, 2000), it seemed logical to evaluate whether the triggering of this receptor might activate signal transduction. As MAPK activation was proved to be crucial in the signal transduction of a large number of membrane receptors (Sebolt-Leopold and Herrera, 2004) we investigated whether TfR2 stimulation might lead to the activation of this kinase cascade. To address this point, we performed crosslinking of TfR2 with the anti-TfR2 mAb G/14C2, stimulation of serum-starved K562 cells with human Tf (h-Tf) and crosslinking of TfR1 with anti-TfR1 mAb. The results showed that TfR2 crosslinking led to the phosphorylation of the extracellular signal-regulated kinases 1 and 2 (ERK1/2), whereas TfR1 crosslinking did not induce similar signalling, as shown by western blot analysis using anti-phospho-ERK1/2 antibody (Fig. 9A, top panel). All control experiments on TfR1 crosslinking using albumin, another serum protein, failed to show any ERK1/2 phosphorylation (Fig. 9A, middle panel), thus indicating that this kinase cascade is specifically induced by TfR2 stimulation. The level of ERK1/2 phosphorylation achieved by TfR2 stimulation corresponded to about 60% of the ERK1/2 phosphorylation induced by phorbol esters (PMA), as indicated by densitometry quantification data (Fig. 9A).

The activation of the ERK/MAPK pathway was also achieved by treating the cells with h-Tf, the natural ligand of TfR2 (Fig. 9A, top panel). This effect was observed using h-Tf at physiological (30 μM) or sub-physiological concentrations (Fig. 9A, bottom panel). Interestingly, bovine transferrin (b-Tf), which is able to bind to human TfR2 but not to human TfR1 (Kawabata et al., 2004) was able to stimulate ERK1/2 as well as h-Tf (Fig. 9A, middle and bottom panels). Control experiments carried with h-Tf a sub-clone of K562 cells, which are TfR2-negative while maintaining TfR1 expression, demonstrated that ERK1/2 activation resulting from transferrin addition is mediated by TfR2 and not by TfR1

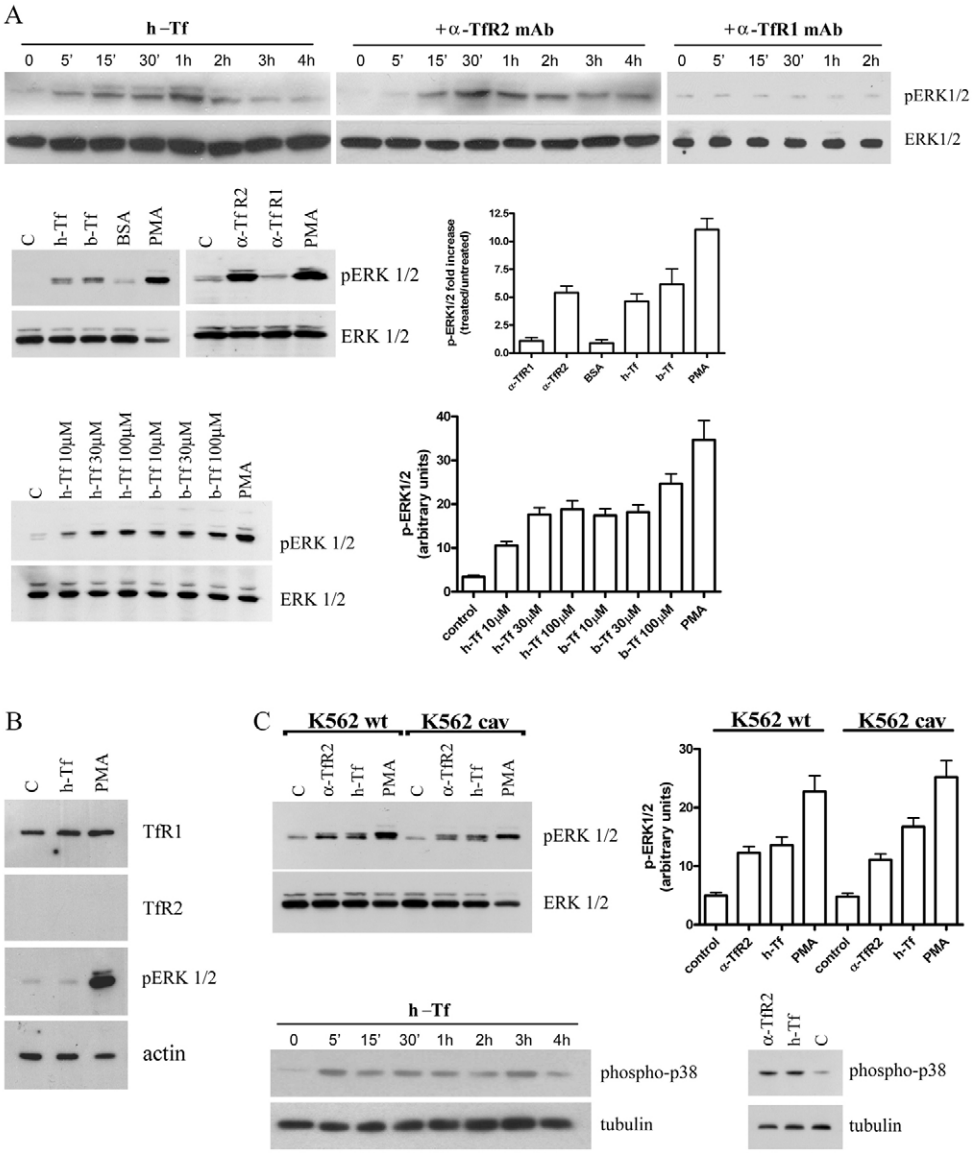

Fig. 9. Activation of ERK1/2 and p38 MAP kinases. (A) Top panel, K562 cells were serum-starved, treated with anti-TfR2 mAb G/14C2, with human transferrin (h-Tf) or with anti-TfR1 mAb for the indicated times and subjected to immunoblotting with anti-phospho-ERK1/2 Ab (pERK1/2). Middle panel: in control experiments, serum-starved K562 cells were exposed to anti-TfR1 Ab (5 minutes, 37°C), bovine serum albumin (BSA; 30 minutes, 37°C), bovine transferrin (b-Tf; 30 μM, 30 minutes, 37°C) and phorbol 12-myristate 13-acetate (PMA; 5 minutes, 37°C). Bottom panel, dose-response curve of ERK1/2 phosphorylation over a physiological and sub-physiological range of h-Tf and b-Tf concentrations. Blots were stripped and reprobed for ERK1/2 to ensure equivalent loading and transfer. (B) A TfR2-negative subclone of K562 cell line was serum-starved, treated with h-Tf (30 μM; 30 minutes, 37°C) and PMA (5 minutes, 37°C) and immunoblotted for TfR1, TfR2, pERK1/2 and actin. (C) Top panel, comparison of the level of ERK1/2 phosphorylation in K562 wt and caveolin-1 transfected K562 cells (K562 cav) exposed to anti-TfR2 (5 minutes, 37°C), h-Tf (30 μM; 30 minutes, 37°C) and PMA (5 minutes, 37°C). Bottom panel, serum-starved K562 cells were treated with anti-TfR2 or h-Tf and used for western analysis to assess the phosphorylation of p38 MAP kinase; blots were stripped and reprobed for tubulin to ensure equivalent loading and transfer. For each treatment, the level of ERK1/2 phosphorylation was quantified by densitometry with the Quantity One program (Bio-Rad) and reported in arbitrary units. Error bars show the range of values obtained in three independent experiments.

(Fig. 9B). In a second set of experiments we compared the level of ERK1/2 activation achieved after TfR2 stimulation with anti-TfR2 and h-Tf in K562 wt and in K562 cav cells. This analysis showed comparable levels of ERK1/2 activation in these two cell lines following stimulation with h-Tf and anti-TfR2 (Fig. 9C, top panel). Thus, although we have proven a strict association between TfR2 and caveolin, the latter did not appear to act as a regulator in TfR2-mediated ERK/MAPK activation.

Finally, we explored whether TfR2 activation might participate in other MAPK-related pathways, for example, via p38 kinase. Experiments carried out under the same conditions as those adopted for the study of ERK1/2 activation showed that TfR2 stimulation with h-Tf as well as with anti-TfR2 mAb led to p38 phosphorylation, with a kinetics comparable to that observed for ERK1/2 (Fig. 9C, bottom panel).

Cholesterol depletion affects TfR2-induced ERK1/2 activation

Cholesterol is crucial for the structural and functional integrity of lipid rafts; the proper cholesterol concentration is required to preserve these microdomains in the liquid-ordered state. In light of the localization of TfR2 in lipid rafts, we investigated the impact of treatment with the cholesterol-depleting drug MBCD on TfR2-induced ERK1/2 activation. Serum-starved K562 cells were treated with MBCD 10 mM for 15 minutes at 37°C before stimulation with anti-TfR2 mAb or PMA. Cells were then lysed and total cell extracts were resolved by SDS-PAGE and immunoblotted against phospho-ERK1/2 (Fig. 10). Pretreatment with MBCD greatly reduced subsequent TfR2-mediated ERK1/2 phosphorylation (Fig. 10, top panel). Incubation of MBCD-treated cells with cholesterol restored an almost normal level of TfR2-mediated ERK1/2 activation (Fig.

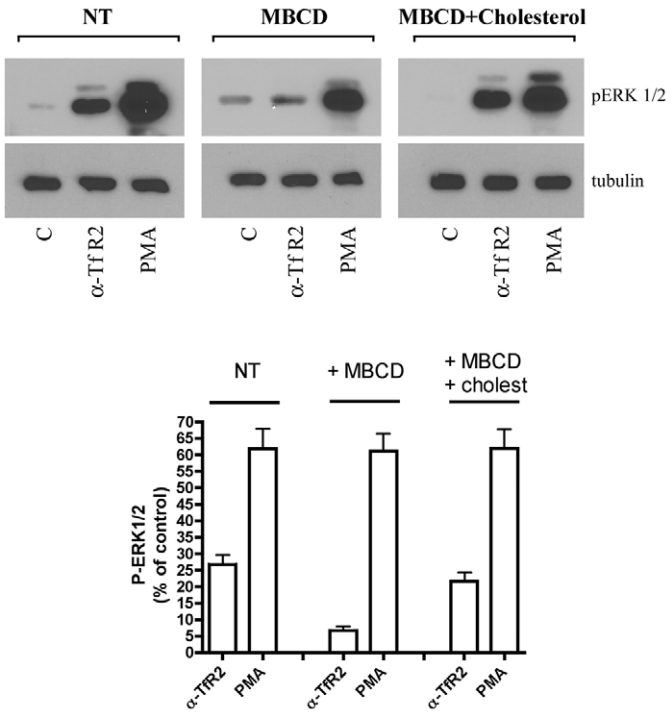

Fig. 10. Effect of cholesterol depletion and repletion on TfR2-mediated ERK1/2 activation. Top panel, serum-starved K562 cells were incubated with or without 10 mM MBCD for 15 minutes at 37°C before treatment with anti-TfR2 mAb or PMA for 5 minutes at 37°C. One aliquot of MBCD-treated cells was incubated with 1 mM water soluble cholesterol. Cells were then collected and lysed. Equal aliquots of total cell lysates from untreated (NT), MBCD-treated (MBCD), and MBCD and cholesterol-treated (MBCD+cholest) cells were resolved by SDS-PAGE and immunoblotted against phospho-ERK1/2. Blots were stripped and reprobed with anti-tubulin Ab to ensure equal protein loading and transfer. Bottom panel, three experiments of this type were evaluated by densitometry to quantify the relative abundance of pERK1/2 induced in response to anti-TfR2 and PMA, normalized with respect to tubulin content and expressed as a percentage of the control (C). Error bars correspond to the range of values obtained in three independent experiments.

10, top panel). These effects were quantified by densitometry from three similar experiments, comparing phosphoERK1/2 signals normalized for tubulin content. As shown in Fig. 10 (bottom panel), cholesterol depletion by MBCD treatment reduced TfR2-induced ERK1/2 phosphorylation by ~80% on average; cholesterol repletion by cholesterol addition to MBCD-treated cells restored ERK1/2 activation to ~80% of the levels observed in untreated (NT) cells. Importantly, MBCD did not modify the PMA-induced ERK1/2 activation (Fig. 10), thus confirming the strong link between TfR2-mediated signalling and its raft association.

Discussion

In this study we demonstrated for the first time that TfR2 is preferentially localized in caveolar microdomains, as indicated by its strict association with membrane lipid rafts. On the other hand, its homologue TfR1 neither interacted with caveolin-1 nor was located in rafts. This finding might have important implications for the understanding of TfR2 function in cell signalling, protein interaction and cellular trafficking. Currently, the functional roles attributed to caveolae and caveolin-1 are quite diverse, ranging from vesicular transport (transcytosis, endocytosis, and potocytosis) and cholesterol homeostasis, to the suppression of cell transformation and the regulation of signal transduction (Parton, 2003). Although we have documented a molecular interaction between caveolin-1 and TfR2, we could not find any evidence for caveolin-1 intervention or regulation on ligand binding or TfR2-induced signalling, as shown in parallel experiments on K562 wt or K562 cav cells.

It is well established that rafts play an important role in signal transduction (Simons and Toomre, 2000; Parton, 2003; Krajewska and Maslowska, 2004). In fact, it was shown that lipid rafts and caveolae form concentrating platforms for individual receptors activated by ligand binding. In general, raft binding recruits proteins to a new micro-environment, where the phosphorylation state can be modified by local kinases and phosphatases, resulting in downstream signalling (Simons and Toomre, 2000).

In line with this finding, we observed that activation of TfR2 by either anti-TfR2 antibody crosslinking or Tf binding induces the activation of ERK1/2 and p38 MAPK pathways, supporting the hypothesis that TfR2 may function as a signalling receptor. The localization of TfR2 in lipid rafts is essential for its signalling. In fact, treatment of K562 cells with the cholesterol-depleting agent MBCD markedly decreased TfR2-induced ERK1/2 activation, which was restored by repletion of cholesterol. These observations are in line with the findings previously reported for other membrane receptors – growth hormone receptor (Yang et al., 2004), insulin-like growth factor receptor (Matthews et al., 2005) and epidermal growth factor receptor (Li et al., 2006). The cell-signalling function is specific for TfR2, whereas TfR1 was unable to generate a similar signalling following interaction with its ligand or anti-TfR1 mAb, as shown by experiments carried out on the $TfR1^{+}/TfR2^{-}$ K562 subclone. The observation that a protein involved in iron metabolism has a particular membrane localization is not novel because previous studies have shown that melanotransferrin, a transferrin homologue that binds iron, is attached to the cell surface via a GPI anchor (Food et al., 1994; Kennard et al., 1995). Interestingly, the function of melanotransferrin does not seem to be restricted to its capacity to act as an iron donor; indeed, membrane-bound melanotransferrin fulfils a regulatory function at the level of condrogenesis, angiogenesis, cell migration and tissue plasminogen activation (Sala et al., 2002; Demeule et al., 2003). Similarly, recent studies on TfR2, mainly based on the analysis of TfR2 mutant mice, indicate that TfR2 may function as a sensor of iron-saturated transferrin in the liver, where it acts upstream of hepcidin in the regulatory pathway of iron homeostasis (Kawabata et al., 2005). This is supported by several observations: (1) both genes are predominantly expressed in the liver (Kawabata et al., 1999; Fleming et al., 2000; Park et al., 2001; Pigeon et al., 2001; Wallace et al., 2005); (2) serum Tf is closely correlated with hepcidin expression in the liver in vivo (Gehrke et al., 2003); (3) expression of both hepcidin mRNA and TfR2 protein are upregulated by iron loading in wild-type mice (Kawabata et al., 2005); (4) urinary hepcidin is low/absent in patients with TfR2 hemochromatosis (Nemeth et al., 2005). Thus, assuming that

TfR2 may function as a hepatic sensor for serum Tf, regulating hepcidin expression or release, Tf-TfR2 interaction may be a crucial event in iron homeostasis in vivo.

The internalization of the Tf-TfR2 complex is not well characterized. Robb et al. show that both TfR2 and TfR1 are localized in the plasma membrane and tubulovesicular vesicles (Robb et al., 2004). Since previous studies have shown that TfR1 is rapidly endocytosed, even in the absence of its ligand, and is largely localized at the level of intracellular compartments (Lamb et al., 1983; Watts, 1985), we have explored the distribution of TfR2 at the level of cell membrane and intracellular organelles. In contrast to TfR1, in K562 cells TfR2 was mainly localized in the plasma membrane, the intracellular pool of the receptor being <10% of the total protein. Subcellular fractionation of K562 cellular lysates on sucrose density gradient provided evidence that TfR2 co-sedimented mainly in the plasma membrane and $Rab5^+$ fractions. This observation is in line with a previous study showing the localization of receptors endocytosed via lipid raft in $Rab5^+$ endosomes (Pelkmans et al., 2004). By contrast, TfR1 was also consistently detected in a fraction co-sedimenting with $Rab11^+/Rab5^-$ endosomes, seemingly representing an endosomic recycling compartment rich in TfR1 (Trischler et al., 1999; Sönnichsen et al., 2000).

An important similarity between TfR2 and TfR1 is that both receptors are actively exocytosed from the cells through the exosomal pathway. The exosomes are small vesicles (60-100 nm) that are released by many cell types and are generated through the fusion of the plasma membrane with multivesicular bodies (MVBs), endocytic structures that contain small vesicles formed from the budding of the membrane of a late endosome into the lumen of the compartment (Théry et al., 2002; Février et al., 2004; Pelchen-Matthews et al., 2004; Johnstone, 2005). The vesicles released through this process are termed exosomes and were initially described in reticulocyte maturation, where their function was to discard plasma membrane proteins that were no longer necessary, such as the TfR1 (Johnstone, 2005). The functions of exosomes have only been partially unveiled, but it is now clear that they serve to remove obsolete membrane proteins and act as messengers in intercellular communication. Exosome secretion has been described for various cell types to be mainly of hematopoietic origin (reviewed by Denzer et al., 2000). Recently, it has been speculated that hepatocytes, being of hematopoietic origin (Lagasse et al., 2000; Nowak et al., 2005), can produce exosomes (Denzer et al., 2000). Finally, exosomes are secreted by many non-hematopoietic cell types, such as intestinal epithelial cells (Van Niel et al., 2001), neuroglial cells (Février et al., 2004) and cancer cells (Wolfers et al., 2001; Riteau et al., 2003; Bard et al., 2004; Hegmans et al., 2004), including hepatoma cell lines HepG2 and HuH-7 (Masciopinto et al., 2004). Biochemical studies have shown that only a select group of macromolecules shed through the exosome pathway, including detergent-soluble plasma membrane proteins such as TfR1, and components of the lipid rafts such as the tetraspanins CD9, CD63 and CD81 (Théry et al., 2002), GPI-anchored proteins such as CD55, CD58, CD59 (Rabesandratana et al., 1998), the Src tyrosine kinase Lyn (Savina et al., 2002; De Gassart et al., 2003), the acylated proteins flotillin-1 and stomatin (De Gassart et al., 2003). The biological significance of exosomes was largely questioned (Couzin, 2005). However, the recent demonstration that exosome-like vesicles are present in human blood plasma supports a physiological role for exosomes in cell-cell or organ-organ communication (Caby et al., 2005).

Here, we show that TfR2, together with CD81, Lyn, TfR1, Lamp-2 and partly caveolin-1, is released in exosomes by both K562 and HepG2 cells. This finding implies that the two membrane receptors TfR1 and TfR2, although located at the level of different membrane domains (TfR1 in detergent-soluble domains and TfR2 in detergent-insoluble domains), co-localize within the cell after their internalization (Robb et al., 2004) and then are released in exosomes.

Studies carried out on the TfR1 show that this membrane receptor may enter either a recycling compartment or an exosome pathway as a result of which molecules interact with its YTRF cytoplasmic domain (Géminard et al., 2004). A similar mechanism could operate for TfR2. Importantly, previous studies show that exosome release by K562 cells is stimulated by diferric transferrin (Savina et al., 2003). Despite some possible co-localization of TfR1 and TfR2 during the first steps of endocytosis from different membrane microdomains, the two proteins clearly diverge during the exocytosis process, as directly supported by the observation that they are present on different exosomes. Thus, $TfR2^+$ exosomes contain CD81, but not TfR1. The presence of the two TfRs on different secretory vesicles might be a consequence of their different physical properties, mainly their solubility, or related to different functions of the $TfR2^+$ and $TfR1^+$ exosomes. It is therefore tempting to speculate that $TfR2^+$ exosomes released from hepatocytes act as extracellular messengers that inform distant cells about iron status. Alternatively, the exocytosis of TfR2-containing exosomes may regulate the liver iron level.

The new finding described here indicating that TfR2 and CD81 associate at the cell membrane, thus possibly sharing a common pathway from membrane lipid rafts to secreted exosomes, deserves further explanation. CD81 is a member of the tetraspanin family, a group of proteins that provide a scaffold facilitating the spatial and temporal engagement of their associated proteins (Hemler, 2003). In line with our observations on TfR2, tetraspanins are localized in membrane microdomains that provide a scaffold for the transmission of exogenous stimuli to intracellular signalling complexes (Hemler, 2003). Furthermore, CD81 is a required receptor for the hepatitis C virus (HCV) (Levy and Shoham, 2005), whose envelope proteins have been found to associate with CD81 in exosomes (Masciopinto et al., 2004). Similarly to our findings on TfR2, the binding of HCV envelope protein E2 to CD81 activates the phosphorylation of ERK1/ERK2 (Mazzocca et al., 2005). Interestingly, TfR2 expression is markedly increased in the liver of patients with chronic hepatitis C (Takeo et al., 2005). This finding was confirmed by Mifuji et al. (Mifuji et al., 2006), showing that TfR2 expression is increased in chronic hepatitis C, usually associated with increased liver iron deposition, but not in chronic hepatitis B, which is more rarely associated with liver iron accumulation. According to these findings, it was suggested that HCV infection might affect the hepatic expression of TfR2, leading to iron accumulation in the liver (Mifuji et al., 2006). These characteristics outline the importance of further studies to assess a functional TfR2/CD81 interaction, which might have strong implications on the exosomal HCV liver infection and on the liver iron overload disease.

In conclusion, the new features of TfR2 described in this study may help to elucidate the close correlation between Tf saturation and hepcidin expression. Possibly, the interaction of holoTf with TfR2 leads to the activation of a signal transduction pathway, which might serve to mediate this relationship. Our studies also indicate that TfR2 is a new raft component sorted in exosomes and through this pathway it could act as an intercellular messenger, carrying a message about cell iron status.

Materials and Methods

Antibodies

Anti-TfR2 monoclonal antibodies (clones G/14C2 and G/14E8) have been reported and characterized in detail in a previous study (Deaglio et al., 2002). Mouse mAb anti-human TfR1 used for western blotting was from Zymed Laboratories (South San Francisco, CA). Mouse mAb anti-human TfR1 used for stimulation in cell signalling experiments was from Sigma (St Louis, MO). Rabbit anti-caveolin-1 (N-20), rabbit polyclonal anti-Lyn and mouse mAb anti-Lamp-2 were obtained from Santa Cruz Biotechnology (Santa Cruz, CA). Mouse mAb anti-human CD81 (clone 1.3.3.22) was from Alexis Biochemicals. Mouse mAb anti-human Golgin-97 was from Molecular Probes. Mouse anti-Rab5 and mouse anti-Rab11 were from BD Biosciences (San Jose, CA). Rabbit anti-phospho-p38 MAPK (T180/Y182), rabbit anti-phospho-ERK1/ERK2 (T202/Y204) and mAb anti-human/mouse/rat ERK1/ERK2 were from R&D Systems. Streptavidin-horseradish peroxidase (HRP)-conjugated Ab was from Pierce.

Cell lines

Erythroleukemic K562 cells and hepatoblastoma HepG2 cells were grown in RPMI 1640 medium containing 10% (v/v) fetal calf serum. Stable expression of caveolin-1 in K562 cells was obtained by a described retroviral-vector-based gene transfer procedure (Parolini et al., 1999).

Confocal microscopy analysis

HepG2 cells were plated on coverslips and left to adhere overnight. Coverslips were stained with mouse mAbs directed against TfR2 or TfR1 (15 minutes at 37°C), followed by a Texas-Red-conjugated goat anti-mouse IgG (Jackson Immunoresearch, West Grove, PA). Cells were then fixed and permeabilized (4% paraformaldehyde, 2% sucrose for 10 minutes at room temperature, plus 0.1% saponin, 10 minutes at room temperature or, alternatively, 100% methanol for 10 minutes at –20°C, plus acetone, 5 seconds at –20°C) and stained with a rabbit polyclonal anti-caveolin-1 (BD Bioscience), followed by a FITC-conjugated anti-rabbit IgG (Jackson ImmunoResearch, West Grove, PA) or with an FITC-conjugated anti-CD81 mAb. Where indicated, stained cells were exposed to Triton X-100 (1% in PBS, 20 minutes) before analysis and nuclei were counterstained with Syto59 (Molecular Probes). All images were acquired using an Olympus 1x71 confocal microscope and processed with Analysis software.

Flow cytometry analysis

K562 cells, untreated or pretreated with 10 mM methyl-β-cyclodextrin (MBCD) for 15 minutes at 37°C, were washed twice in PBS and then incubated in the presence of 1 μg/ml anti-TfR2 mAb (G/14E8) or 1 μg/ml anti-CD81 mAb (clone 1.3.3.22) or 1 μg/ml irrelevant mouse IgG for 30 minutes at 4°C, washed twice in cold PBS and then incubated with affinity-purified goat anti-mouse IgGs diluted 1:40 (Dakopatts, Copenaghen, Denmark). After two additional washes in PBS, the cells were analyzed in a FACS SCAN flow cytometer (Becton Dickinson, San José, CA). For TfR1 labeling, these cells were incubated with PE-conjugated anti-TfR1 Ab (Becton-Dickinson, USA).

In some experiments, before labeling with antibodies, K562 cells were pretreated with 10 mM methyl-β-cyclodextrin (MBCD) for 15 minutes at 37°C: this treatment allows disruption of lipid rafts by cholesterol depletion. For detergent-sensitivity analysis, an aliquot of labeled cells with anti-TfR2, anti-CD81 or anti-TfR1, was incubated for 5 minutes at 25°C with PBS containing 0.2% Triton X-100 and then reanalyzed by flow cytometry. It was previously shown that this procedure allows one to distinguish detergent-soluble and detergent-resistant (raft-associated) membrane proteins (Gombos et al., 2004).

In some experiments, to remove membrane-bound transferrin receptors (Watts, 1985), K562 and HepG2 cells have been incubated for 60 minutes at 4°C in the presence of trypsin (500 μg/ml), washed with PBS containing 10% FCS and then labeled with anti-TfR1 and anti-TfR2 mAbs. To detect both membrane-bound and intracellular TfRs, cells were fixed and permeabilized using Cytofix/Cytoperm (BD/Pharmingen, Mountain View, CA), and then labeled and processed following the protocol recommended by the supplier.

Isolation of caveolae-enriched membrane fractions

Caveolae-enriched membrane fractions were isolated according to standard protocols (Lisanti et al., 1993; Parolini et al., 1996). Briefly, the cell pellet was dissolved in 0.75 ml MES-buffered saline (25 mM MES pH 6.5, 150 mM NaCl) containing 1% Triton X-100 at 4°C. Cell lysate was Dounce homogenized, adjusted to 40% sucrose and placed at the bottom of an ultracentrifuge tube. A 5-30% linear sucrose gradient was then placed above the homogenate and the mixture was centrifuged at 45,000 rpm for 16 hours at 4°C in an SW60 rotor (Beckman Instruments, Palo Alto, CA). The caveolar fractions are visible as a light-scattering band migrating at approximately 20% sucrose. Twelve 0.375 ml fractions were collected from the top to the bottom of the gradient, separated by SDS-PAGE and subjected to immunoblot analysis. Fractions 1 and 2 generally do not contain proteins and thus were not subjected to SDS-PAGE. Fraction 12 represents the nuclear portion.

Purification and biotinylation of plasma membrane proteins

To purify plasma membrane proteins, HepG2 and K562 cav cells were lysed with 10 mM Tris-HCl pH 7.4, 1 mM EDTA, for 30 minutes at 4°C then centrifuged at 1000 ***g*** to remove nuclei. The supernatant was then centrifuged at 30,000 ***g*** for 60 minutes to isolate membrane portions (pellet) from cytosolic proteins (supernatant).

For biotin labeling, HepG2 and K562 cav cells were washed three times with PBS without calcium and magnesium and incubated with water-soluble Sulfo-NHS-biotin (Calbiochem) (0.5 mg/ml; 30 minutes at 4°C). The cells were then processed to obtain PM as previously described, or LDTI domains by density gradient centrifugation.

Subcellular fractionation

K562 cells (50-100×10^6) were collected by centrifugation, washed twice with PBS, resuspended in 10 mM Tris-HCl pH 7.4, 1 mM EDTA, 100 mM KCl, transferred to a 15 ml nitrogen cavitation bomb and held in 400 psi N_2 pressure for 30 minutes. The cavitated cells were disrupted further with a dounce homogenizer and the resulting lysate was centrifuged at 1000 ***g*** to remove nuclei, intact cells and large cellular debris. The postnuclear supernatant was layered on top of a series of sucrose steps (38%, 30%, 20%) and fractionated in an SW60 rotor at 30,000 rpm for 2 hours at 4°C. Four fractions were collected from the top of the tube and the pellet (fraction 5) was resuspended in Tris-HCl-EDTA-KCl.

Isolation of exosomes

Exosomes were prepared according to a procedure previously described (Vidal and Stahl, 1993). Briefly, exosomes were collected from 70 ml of confluent K562 or HepG2 cells. The culture media were collected on ice, centrifuged at 3500 rpm for 20 minutes in a GH-3.8 rotor to sediment the cells, and then centrifuged at 11,000 rpm for 20 minutes in an SW41 rotor to remove cellular debris. Exosomes were separated from the supernatant by centrifugation at 33,000 rpm for 1 hour in an SW41 rotor (Beckman Instruments, Palo Alto, CA). The exosome pellet was washed once in a large volume of PBS and finally resuspended in PBS for further analysis.

Western blot analysis and immunoprecipitation

Protein samples were resolved by 7.5% SDS-PAGE under reducing and denaturing conditions and transferred to nitrocellulose filter. The blots were blocked using 5% non-fat dry milk in TBST (10 mM Tris-HCl pH 8.0, 150 mM NaCl, 0.1% Tween 20) for 1 hour at room temperature, followed by incubation with primary antibodies. After washing with TBST, the filters were incubated with the appropriate horseradish-peroxidase-conjugated secondary antibodies (Bio-Rad) for 1 hour at room temperature. Immunoreactivity was revealed by using an ECL detection kit (Pierce).

For TfR2 and TfR1 immunoprecipitation experiments, LDTI fractions collected from sucrose gradient centrifugation of biotinylated HepG2 cells were used. For the immunoprecipitation of CD81, purified exosomes and LDTI domains prepared from K562 cav cells were used. Protein samples were precleared with 30 μl of a 50% slurry protein A/G-agarose (Pierce) in 0.5 ml of lysis buffer (150 mM NaCl, 10 mM Tris-HCl, pH 7.4, 1 mM EDTA, 0.5% Nonidet P-40, 1% Triton X-100, 60 mM octylglucoside, supplemented with a cocktail of protease inhibitors) for 1 hour at 4°C. Anti-TfR2, anti-TfR1 or anti-CD81 antibodies were then added to the sample and kept overnight at 4°C, followed by incubation with pre-washed beads (40 μl) for 1 hour at 4°C. The beads were then spun down and washed four times with lysis buffer, resuspended in 30 μl of reducing SDS-PAGE sample buffer, boiled and spun down. The supernatant was loaded on a 7.5% SDS-PAGE and subjected to western blotting analysis. To control for specificity, the antibodies alone were immunoprecipitated in the same way as the protein samples. In some experiments, exosomes were immunoprecipitated as described above with anti-TfR2 and anti-CD81 mAbs, in the absence of detergents.

Stimulation of TfR2

In a first set of experiments, TfR2 stimulation was performed by the crosslinking of TfR2 with the anti-TfR2 mAb G/14C2. K562 cells were serum-starved overnight, pre-incubated for 2 hours at 37°C with 1 μM ST1571 (Gleevec, Novartis) and then incubated for 10 minutes on ice with anti-TfR2 mAb (1 μg/10^5 cells), then transferred to 37°C for the indicated times. As a control, the same number of cells

was left untreated or treated with an anti-TfR1 mAb (Clone DF 1513, Sigma). The pre-treatment of K562 cells with the tyrosine kinase inhibitor ST1571 was important to obtain a reproducibly very low level of constitutive MAPK activation in unstimulated cells. In a second set of experiments, K562 cells were incubated with purified human holotransferrin (h-Tf) 10, 30 or 100 μM at 37°C. In some experiments the cells were incubated with purified bovine holotransferrin (b-Tf) 10, 30 or 100 μM at 37°C. As a control, the same number of cells was incubated with bovine serum transferrin (BSA). Both transferrin preparations were purchased from Sigma. Where indicated, h-Tf was used to stimulate a clone of K562 cells, which are TfR2 negative while retaining their TfR1 expression. In all types of analysis, to terminate the stimulation, cells were cooled to 4°C and washed twice with cold PBS. The cell pellet was finally boiled in SDS-PAGE reducing sample buffer and subjected to immunoblot analysis. In some experiments, serum-starved K562 cells were incubated with 10 mM MBCD for 15 minutes at 37°C before treatment with anti-TfR2 mAb or PMA for 5 minutes at 37°C. One aliquot of MBCD-treated cells was incubated with 1 mM water-soluble cholesterol, before TfR2 stimulation. Cells were finally lysed and analyzed for ERK1/2 activation.

This study was partially supported by a FIRB grant year 2003 (Grant RBNE03FMCJ_002) from the Italian Ministry for University and Research (to M.S.). K.F. and C.R. were recipients of postdoctoral and PhD fellowships from FIRB.

References

Bard, M. P., Hegmans, J. P., Hemmes, A., Luider, T. M., Willemsen, R., Severijnen, L. A., Van Meerbeeck, J. P., Burgers, S. A., Hoogsteden, H. C. and Lambrecht, B. N. (2004). Proteomic analysis of exosomes isolated from human malignant pleural effusions. *Am. J. Respir. Cell Mol. Biol*. **31**, 114-121.

Blanchard, N., Lankar, D., Faure, F., Regnault, A., Dumont, C., Raposo, G. and Hivroz, C. (2002). TCR activation of human T cells induce the production of exosomes bearing the TCR/CD3/zeta complex. *J. Immunol.* **168**, 3235-3241.

Caby, M. P., Lankar, D., Vincendeau-Scherrer, C., Raposo, G. and Bonerrot, C. (2005). Exosomal-like vesicles are present in human blood plasma. *Int. Immunol*. **17**, 879-887.

Camaschella, C., Roetto, A., Cali, A., De Gobbi, M., Garozzo, G., Carella., M., Majorano, N., Totaro, A. and Gasparini, P. (2000). The gene TFR2 is mutated in a new type of hemochromatosis mapping to 7q22. *Nat. Genet*. **25**, 14-15.

Couzin, J. (2005). The ins and outs of exosomes. *Science* **308**, 1862-1863.

De Gassart, A., Géminard, C., Février, B., Raposo, G. and Vidal, M. (2003). Lipid raft-associated protein sorting in exosomes. *Blood* **102**, 4336-4344.

Deaglio, S., Capobianco, A., Cali, A., Bellora, F., Alberti, F., Righi, L., Sapino, A., Camaschella, C. and Malavasi, F. (2002). Structural, functional, and tissue distribution analysis of human transferrin receptor-2 by murine monoclonal antibodies and a polyclonal antiserum. *Blood* **100**, 3782-3789.

Demeule, M., Bertrand, Y., Michaud-Levesque, J., Jodoin, J., Rolland, Y., Gabathuler, R. and Béliveau, R. (2003). Regulation of plasminogen activation: a role for melanotransferrin (p97) in cell migration. *Blood* **102**, 1723-1731.

Denzer, K., Kleijmeer, M. J., Heijnen, H. F. G., Stoorvogel, W. and Geuze, H. J. (2000). Exosome: from internal vesicle of the multivesicular body to intercellular signaling device. *J. Cell Sci.* **113**, 3365-3374.

Escola, J. M., Kleijmeer, M. J., Stoorvogel, W., Griffith, J. M., Yoshie, O. and Geuze, H. J. (1998). Selective enrichment of tetraspan proteins on the internal vesicles of multivesicular endosomes and on exosomes secreted by human B-lymphocytes. *J. Biol. Chem.* **273**, 20121-20127.

Février, B., Vilette, D., Archer, F., Loew, W., Faigle, W., Vidal, M., Laude, H. and Raposo, G. (2004). Cells release prions in association with exosomes. *Proc. Natl. Acad. Sci. USA* **101**, 9683-9688.

Fleming, R. E., Migas, M. C., Holden, C. C., Waheed, A., Britton, R. S., Tomatsu, S., Bacon, B. R. and Sly, W. S. (2000). Transferrin receptor 2, continued expression in mouse liver in the face of iron overload and in hereditary hemochromatosis. *Proc. Natl. Acad. Sci. USA* **97**, 2214-2219.

Food, M. R., Rothenberger, S., Gabathuler, R., Haidl, I. D., Reid, G. and Jefferies, W. A. (1994). Transport and expression in human melanomas of a transferrin-like glycophosphatidylinositol-anchored protein. *J. Biol. Chem.* **269**, 3034-3040.

Gehrke, S. G., Kulaksiz, H., Hermann, T., Riedel, H. D., Bents, K., Veltkamp, C. and Stremmel, W. (2003). Expression of hepcidin in hereditary hemochromatosis: evidence for a regulation in response to serum transferrin saturation and non-transferrin-bound iron. *Blood* **102**, 371-376.

Géminard, C., De Gassart, A., Blanc, L. and Vidal, M. (2004). Degradation of AP2 during reticulocyte maturation enhances binding of Hsc70 and Alix to a common site on TfR for sorting into exosomes. *Traffic* **5**, 181-193.

Glockner, G., Scherer, S., Schattevoy, R., Boright, A., Weber, J., Tsui, L. C., Boright, A., Weber, J., Tsui, L. C. and Rosenthal, A. (1998). Large-scale sequencing of two regions in human chromosome 7q22: analysis of 650 Kb of genomic sequence around the EPO and CUTL1 loci reveals 17 genes. *Genome Res*. **8**, 1060-1073.

Gombos, I., Bacsó, Z., Detre, C., Nagy, H., Goda, K., Andrásfalvy, M., Szabó, G. and Matkó, J. (2004). Cholesterol sensitivity of detergent resistance: a rapid flow cytometric test for detecting constitutive or induced raft association of membrane proteins. *Cytometry A* **61**, 117-126.

Griffiths, W. J. H. and Cox, T. M. (2003). Co-localization of the mammalian hemochromatosis gene product (HFE) and a newly identified transferrin receptor (TfR2) in intestinal tissue and cells. *J. Histochem*. **51**, 613-623.

Gutwein, P., Stoeck, A., Riedle, S., Gast, D., Runz, S., Condon, T. P., Marmé, A., Phong, M. C., Linderkamp, O., Skorokhod, A. et al. (2005). Cleavage of L1 in exosomes and apoptotic membrane vesicles released from ovarian carcinoma cells. *Clin. Cancer Res*. **11**, 2492-2501.

Hegmans, J. P., Bard, M. P., Hemmes, A., Luider, T. M., Kleijmeer, M. J., Prins, J. B., Zitvogel, L., Burgers, S. A., Hoogsteden, H. C. and Lambrecht, B. N. (2004). Proteomic analysis of exosomes secreted by human mesothelioma cells. *Am. J. Pathol.* **164**, 1807-1815.

Hemler, M. E. (2003). Tetraspanin proteins mediate cellular penetration, invasion, and fusion events and define a novel type of membrane microdomain. *Annu. Rev. Cell Dev. Biol*. **19**, 397-422.

Johnson, M. B. and Enns, C. A. (2004). Diferric transferrin regulates transferrin receptor 2 protein stability. *Blood* **104**, 4287-4293.

Johnstone, R. M. (2005). Revisiting the road to the discovery of exosomes. *Blood Cells Mol. Dis*. **34**, 214-219.

Kawabata, H., Yang, R., Hirama, T., Vuong, P. T., Kawano, S., Gombart, A. F. and Koeffler, H. P. (1999). Molecular cloning of transferrin receptor 2. A new member of the transferrin receptor-like family. *J. Biol. Chem*. **274**, 20826-20832.

Kawabata, H., Germain, R. S., Vuong, P. T., Nakamaki, T., Said, J. W. and Koeffler, H. P. (2000). Transferrin receptor 2-alpha supports cell growth both in iron-chelated cultured cells and in vivo. *J. Biol. Chem.* **275**, 16618-16625.

Kawabata, H., Germain, R. S., Ikezoe, T., Tong, X., Green, E. M., Gombart, A. F. and Koeffler, H. P. (2001). Regulation of expression of murine transferrin receptor 2. *Blood* **98**, 1949-1954.

Kawabata, H., Tong, X., Kawanami, T., Wano, Y., Hirose, Y., Sugai, S. and Koeffler, H. P. (2004). Analyses for binding of the transferrin family of proteins to the transferrin receptor 2. *Br. J. Haematol*. **127**, 464-473.

Kawabata, H., Fleming, R. E., Gui, D., Moon, S. Y., Takayuki, S., O'Kelly, J., Umehara, Y., Wano, Y., Said, J. W. and Koeffler, H. P. (2005). Expression of hepcidin is down-regulated in TfR2 mutant mice manifesting a phenotype of hereditary hemochromatosis. *Blood* **105**, 376-381.

Kennard, M. L., Richardson, D. R., Gabathuler, R., Ponka, P. and Jefferies, W. A. (1995). A novel iron uptake mechanism mediated by GPI-anchored human p97. *EMBO J.* **14**, 4178-4186.

Krajewska, W. M. and Maslowska, I. (2004). Caveolins: structure and function in signal transduction. *Cell. Mol. Biol. Lett*. **9**, 195-220.

Lagasse, E., Connors, H., Al-Dhalimy, M., Reitsma, M., Dohse, M., Osborne, L., Wang, X., Finegold, M., Weissman, I. L. and Grompe, M. (2000). Purified hematopoietic stem cells can differenziate into hepatocytes in vivo. *Nat. Med*. **6**, 1229-1234.

Lamb, J. E., Ray, F., Ward, J. H., Kusher, J. P. and Kaplan, J. (1983). Internalization and subcellular localization of transferrin and transferrin receptors in HeLa cells. *J. Biol. Chem*. **258**, 8751-8758.

Levy, S. and Shoham, T. (2005). The tetraspanin web modulates immune-signalling complexes. *Nat. Rev. Immunol*. **5**, 136-148.

Li, Y. C., Park, M. J., Ye, S. K., Kim, C. W. and Kim, Y. N. (2006). Elevated levels of cholesterol-rich lipid rafts in cancer cells are correlated with apoptosis sensitivity induced by cholesterol-depleting agents. *Am. J. Pathol*. **168**, 1107-1118.

Lisanti, M. P., Tang, Z. L. and Sargiacomo, M. (1993). Caveolin forms a hetero-oligomeric protein complex that interacts with an apical GPI-linked protein: implications for the biogenesis of caveolae. *J. Cell Biol*. **123**, 595-604.

Masciopinto, F., Giovani, C., Campagnoli, S., Galli-Stampino, L., Colombatto, P., Brunetto, M., Yen, B. T. S., Houghton, M., Pileri, P. and Abrignani, S. (2004). Association of hepatitis C virus envelope proteins with exosomes. *Eur. J. Immunol*. **34**, 2834-2842.

Matthews, L. C., Taggart, M. J. and Westwood, M. (2005). Effect of cholesterol depletion on mitogenesis and survival: the role of caveolar and noncaveolar domains in insuline-like growth factor-mediated cellular function. *Endocrinology* **146**, 5463-5473.

Mazzocca, A., Cappadona Sciammetta, S., Carloni, V., Cosmi, L., Annunziato, F., Harada, T., Abrignani, S. and Pinzani, M. (2005). Binding of Hepatitis C Virus envelope protein E2 to CD81 up-regulates matrix metalloproteinase-2 in human hepatic stellate cells. *J. Biol. Chem*. **280**, 11329-11339.

Mifuji, R., Kobayashi, Y., Ma, N., Quing, Q. L., Urawa, N., Horiike, S., Iwasa, M., Kaito, M., Malavasi, F. and Adachi, Y. (2006). Role of transferrin receptor 2 in hepatic accumulation of iron in patients with chronic hepatitis C. *J. Gastroenterol. Hepatol.* **21**, S144-S151.

Nemeth, E., Roetto, A., Garozzo, G., Ganz, T. and Camaschella, C. (2005). Hepcidin is decreased in TfR2 hemochromatosis. *Blood* **105**, 1803-1806.

Nguyen, D. G., Booth, A., Gould, S. J. and Hildreth, J. E. (2003). Evidence that HIV budding in primary macrophages occurs through the exosome release pathway. *J. Biol. Chem.* **278**, 52347-52354.

Nowak, G., Ericzon, B. G., Nava, S., Jaksach, M., Westgren, M. and Sumitran-Holgersson, S. (2005). Identification of expandable human hepatic progenitors which differentiate into mature hepatic cells in vivo. *Gut* **54**, 972-979.

Park, C. H., Valore, E. V., Waring, A. J. and Ganz, T. (2001). Hepcidin, a urinary antimicrobial peptide synthesized in the liver. *J. Biol. Chem.* **276**, 7806-7810.

Parolini, I., Sargiacomo, M., Lisanti, M. P. and Peschle, C. (1996). Signal transduction and glycophosphatidylinositol-linked proteins (lyn, lck, CD4, CD45, G proteins, and

CD55) selectively localize in Triton-insoluble plasma membrane domains of human leukemic cell lines and normal granulocytes. *Blood* **87**, 3783-3794.

Parolini, I., Sargiacomo, M., Galbiati, F., Rizzo, G., Grignani, F., Engelman, J. A., Okamoto, T., Ikezu, T., Sherer, P. E., Mora, R. et al. (1999). Expression of caveolin-1 is required for the transport of caveolin-2 to the plasma membrane. Retention of caveolin-2 at the level of the Golgi complex. *J. Biol. Chem.* **274**, 25718-25725.

Parton, R. G. (2003). Caveolae – from ultrastructure to molecular mechanism. *Nat. Rev. Mol. Cell Biol*. **4**, 162-167.

Pelchen-Matthews, A., Raposo, G. and Marsh, M. (2004). Endosomes, exosomes and Trojan viruses. *Trends Microbiol*. **12**, 310-316.

Pelkmans, L., Burli, T., Zerial, M. and Helenius, A. (2004). Caveolin-stabilized membrane domains as multifunctional transport and sorting devices in endocytic membrane traffic. *Cell* **118**, 767-780.

Pigeon, C., Ilyn, G., Courselaud, B., Leroyer, P., Turlin, B., Brissot, P. and Loreal, O. (2001). A new mouse liver-specific gene, encoding a protein homologous to human antimicrobial peptide hepcidin, is overexpressed during iron overload. *J. Biol. Chem*. **276**, 7811-7819.

Rabesandratana, H., Toutant, J. P., Reggio, H. and Vidal, M. (1998). Decay-accelerating factor (CD55) and the membrane inhibitor of reactive lysis (CD59) are released within exosomes during in vitro maturation of reticulocytes. *Blood* **91**, 2573-2580.

Riteau, B., Faure, F., Menier, C., Viel, S., Carosella, E. D., Amigorena, S. and Rouas-Freiss, N. (2003). Exosomes bearing HLA-G are secreted by melanoma cells. *Hum. Immunol*. **64**, 1064-1072.

Robb, A. D., Ericsson, M. and Wessling-Resnick, M. (2004). Transferrin receptor 2 mediates a biphasic pattern of transferrin uptake associated with ligand delivery to multivesicular bodies. *Am. J. Physiol. Cell Physiol*. **287**, C1768-C1775.

Roetto, A., Daraio, F., Alberti, F., Porporato, P., Calì, A., De Gobbi, M. and Camaschella, C. (2002). Hemochromatosis due to mutations in transferrin receptor 2. *Blood Cells Mol. Dis*. **29**, 465-470.

Sala, R., Jefferies, W. A., Walker, B., Yang, J., Tiong, J., Law, S. K., Carlevaro, M. F., Di Marco, E., Vacca, A., Cancedda, R. et al. (2002). The human melanoma associated protein melanotransferrin promotes endothelial cell migration and angiogenesis in vivo. *Eur. J. Cell Biol.* **81**, 599-607.

Sargiacomo, M., Lisanti, M. P., Graeve, L., Le Bivic, A. and Rodriguez-Boulan, E. (1989). Integral and peripheral protein composition of the apical and basolateral membrane domains in MDCK cells. *J. Membr. Biol*. **107**, 277-286.

Savina, A., Vidal, M. and Colombo, M. I. (2002). The exosome pathway in K562 cells is regulated by Rab11. *J. Cell Sci.* **115**, 2505-2515.

Savina, A., Furlàn, M., Vidal, M. and Colombo, M. I. (2003). Exosome release is regulated by a calcium-dependent mechanism in K562 cells. *J. Biol. Chem.* **278**, 20083-20090.

Sebolt-Leopold, J. S. and Herrera, R. (2004). Targeting the mitogen-activated protein kinase cascade to treat cancer. *Nat. Rev. Cancer* **4**, 937-947.

Simons, K. and Toomre, D. (2000). Lipid rafts and signal transduction. *Nat. Rev. Mol. Cell Biol*. **1**, 31-39.

Sönnichsen, B., De Renzis, S., Nielsen, E., Rietdorf, J. and Zerial, M. (2000). Distinct membrane domains on endosomes in the recycling pathway visualized by multicolour imaging of Rab4, Rab5, and Rab11. *J. Cell Biol.* **149**, 901-913.

Takeo, M., Kobayashi, Y., Fujita, N., Urawa, N., Iwasa, M., Horiike, S., Tanaka, H., Kaito, M. and Adachi, Y. (2005). Upregulation of transferrin receptor 2 and ferroportin 1 mRNA in the liver of patients with chronic hepatitis C. *Hepatology* **20**, 562-569.

Théry, C., Boussac, M., Véron, P., Ricciardi-Castagnoli, P., Raposo, G., Garin, J. and Amigorena, S. (2001). Proteomic analysis of dendritic cell-derived exosomes: a secreted subcellular compartment distinct from apoptotic vesicles. *J. Immunol*. **166**, 7309-7318.

Théry, C., Zitvogel, L. and Amigorena, S. (2002). Exosomes: composition, biogenesis and function. *Nat. Rev. Immunol*. **2**, 569-579.

Trischler, M., Stoorvogel, W. and Ullrich, O. (1999). Biochemical analysis of distinct Rab5- and Rab11-positive endosomes along the transferrin pathway. *J. Cell Sci.* **112**, 4773-4783.

Van Niel, G., Raposo, G., Candalh, C., Boussac, M., Hershberg, R., Cerf-Bensussan, N. and Heyman, M. (2001). Intestinal epithelial cells secrete exosome-like vesicles. *Gastroenterology* **121**, 337-349.

Vidal, M. J. and Stahl, P. D. (1993). The small GTP-binding proteins Rab4 and ARF are associated with vesicles released during reticulocyte maturation. *Eur. J. Cell Biol*. **60**, 261-267.

Wallace, D. F., Summerville, L., Lusby, P. E. and Subramaniam, V. N. (2005). First phenotypic description of transferrin receptor 2 knockout mouse, and the role of hepcidin. *Gut* **54**, 980-986.

Watts, C. (1985). Rapid endocytosis of the transferrin receptor in the absence of bound transferrin. *J. Cell Biol*. **100**, 633-637.

Wolfers, J., Lozier, A., Raposo, G., Regnault, A., Théry, C., Masurier, C., Flement, C., Pouzieux, S., Faure, S., Tursz, T. et al. (2001). Tumor-derived exosomes are a source of shared tumor rejection antigens for CTL cross-priming. *Nat. Med*. **7**, 297-303.

Yang, N., Huang, Y., Jiang, J. and Frank, S. J. (2004). Caveolar and lipid raft localization of the growth hormone receptor and its signalling. *J. Biol. Chem*. **279**, 20898-20905.